



## COPPER SEEDS FOR HIGH QUALITY ELECTRODEPOSITION OF COBALT-RICH ALLOYS NANOSTRUCTURES ON SILICON

Edna R. Spada<sup>1</sup>, Marta E. R. Dotto<sup>2</sup>, Maria L. Sartorelli<sup>3</sup> & Fernando R. de Paula<sup>\*4</sup>

<sup>1</sup>Instituto de Física de São Carlos, Universidade de São Paulo, Caixa Postal 369, 13560-970, São Carlos, SP, Brazil

<sup>2&3</sup>Laboratório de Sistemas Nanoestruturados, Departamento de Física, Universidade Federal de Santa Catarina, Caixa Postal 476, 88040-900, Florianópolis, SC, Brazil

<sup>\*4</sup>Departamento de Física e Química, Faculdade de Engenharia, Universidade Estadual Paulista – UNESP, Campus IlhaSolteira, CEP 15385-000, IlhaSolteira, SP, Brazil

DOI: 10.5281/zenodo.1097040

**Keywords:** electrodeposition, magnetic alloy, thin films, nanosphere lithography

### Abstract

We report the electrodeposition (ED) of cobalt-rich alloy films on n-type Si (100) substrates in aqueous solution. A small amount of copper sulfate in the bath improved the quality of cobalt-rich films. The bath proved to be appropriate for the production of electrodeposited magnetic antidot structures prepared by nanosphere lithography (NSL) technique. X-ray measurements indicate a mixture of hcp and fccCoCu structures and firm texture in the (001) hcp and (111) fcc direction. Magnetic behavior was shown to be dependent on the thickness, which directly affects the domain wall pinning and the presence of superparamagnetism.

### Introduction

The electrochemical deposition is an attractive method that allows the production of metal films at room temperature and atmospheric pressure. This process is an adequate alternative for molecular beam epitaxy (MBE) or sputtering. In the perspective of industrial-scale fabrication and mass production, electrodeposition is attractive due to its relatively low cost, simplicity, high deposition rate, extended surface, and the possibility of broad scale application. Depending on the conditions at preparation, (*i.e.*, electrolyte composition, pH solution, temperature, current density, and presence of additives) films with different morphological and structural properties can be obtained [1-4]. Additives, such as saccharine and trisodium citrate, may act as inhibitors of crystal growth and catalyst, leading to bright deposits and decreasing the overpotential metal electrodeposition.

The high quality of magnetic films on silicon semiconductor substrate using electrodeposition technique is attracting the attention to electronic applications; because it enables the connection of silicon technology with magnetic properties, allowing the information storage and processing in one single electronic device. In this respect, cobalt is one of the most crucial ferromagnetic materials to produce magnetic thin film; however, one of the leading concerns is the preparation of films with low-coercivity properties for electronic applications [5-9]. Cobalt is a ferromagnetic material at a Curie temperature of 1,388 K and ~1.72 Bohr magnetons per atom, and can be found in two stable forms: bulk hexagonal-close-packed (hcp) and face-center-cubic (fcc) (below 698 K and at high temperatures, respectively) [10]. Although hcp is its stable form at room temperature, cobalt electrodeposited often contain a mixture of both hcp and fcc, which can be obtained by selecting the bath and the electrodeposition conditions [11].

Our research focuses on the electrodeposition of cobalt-rich films on silicon substrate. The electrolytic bath developed contains additive trisodium citrate and a small concentration of copper. The high quality films obtained by electrodeposition are of interest due to their potential applications in high-density magnetic data storage media, flux pinning in superconductors, and spin transport mechanism. Films obtained electrochemically are also ideal for nanostructuring with NSL [12-14]. When the NSL is used, the formation of a regularly ordered structure is strongly dependent on the quality of films grown on the substrate. The use of these techniques to produce magnetic antidot structures is particularly interesting because of its applications in high-density



## INTERNATIONAL JOURNAL OF RESEARCH SCIENCE & MANAGEMENT

magnetic data storage and for the understanding of fundamental magnetism in confined geometries, such as magnetization and spintronics [15-18].

### Experimental section

Experimental electrodeposition was performed at room temperature in a dark chamber using a three-electrode cell with AUTOLAB PGSTAT302N galvanostat/potentiostat. The working electrode single-sided polished circular-type Si(100)-oriented wafers with a resistivity of 5-10  $\Omega\text{cm}$  at room temperature. An adhesive tape was used to mask off all the substrate except for the circular area of 0.496  $\text{cm}^2$  on which the deposition was desired. Native oxide ( $\text{SiO}_2$ ) was removed with HF etching before the experiments. A gallium-indium alloy was used on the backside of the Si wafer to improve the Ohmic contact. Platinum foil and a standard saturated calomel electrode (SCE) were used as the counter and reference electrode, respectively. All potentials are given concerning to reference electrode.

The electrodeposition of cobalt-rich films was performed in a solution containing 300 mM of cobalt(II)sulfate heptahydrate ( $\text{CoSO}_4 \cdot 7\text{H}_2\text{O}$ ) and 3 mM of copper(II) sulfate pentahydrate ( $\text{CuSO}_4 \cdot 5\text{H}_2\text{O}$ ) in filtered deionized water. As complexing agent was used 300 mM sodium citrate ( $\text{C}_6\text{H}_5\text{Na}_3\text{O}_7 \cdot 5\text{H}_2\text{O}$ ). Voltammetric analysis was carried out at  $10\text{mVs}^{-1}$  scanning to negative potentials at first. Only one cycle was run in each voltammetric experiment. The films were grown in natural pH of 5.5 by applying a cathodic potential of -1.1V/SCE with a nominal thickness of films ranging between 5 and 500 nm. After deposition, all samples were removed from the electrochemical cell, rinsed thoroughly with distilled water, and dried in a nitrogen flux.

Atomic Force Microscopy (AFM) analysis was performed on a NanosurfFlexAFM microscope operating in tapping mode under ambient conditions with a scan rate of 1.0 Hz and 512 pixels x 512 pixels was the image's resolution, and a tip TAP190Al-G model was used. The lateral size of acquired images was a set of distinct sizes (10, 20, 45 and 90  $\mu\text{m}$ ), but only images with 10  $\mu\text{m}$  of lateral size are shown. The AFM images were treated using the 5.0 WSxM Develop 7.0 software.

The crystalline structure was analyzed by X-ray diffraction (XRD) on a diffractometer model X'Pert Pro Multi-Purpose, PanAnalytical, where the X-ray source was Cu  $K_{\alpha 1}$  radiation ( $\lambda = 1.540562 \text{ \AA}$ ), powered at 40 kV and 30 mA. Measurements were performed in  $2\theta$  configuration with the incident beam fixed at  $12^\circ$  and  $2\theta$  between  $30^\circ$  to  $80^\circ$ . In order to increase the signal-noise ratio, each measure presented is the sum of 30 scans. The composition of the films was obtained by Energy Dispersive X-ray Microanalysis (EDX) and Surface morphology images were obtained at acquisition modes of secondary (SE) on a Phillips XL30 scanning electron microscope (SEM). The magnetic characterizations were performed at room temperature in a vibrating sample magnetometer (VSM model EV9 Microsense) in the field range of  $\pm 10 \text{ kOe}$ .

## Results and discussion

### 1. Electrochemical characterization

The electrodeposition potential of films on silicon (100) was determined by the analysis of the voltammetric curves obtained at a scan rate of  $10 \text{ mVs}^{-1}$ . Fig. 1a shows the partial voltammetric curves of three different solutions. The reduction of cobalt begins around -0.95 V/SCE in a solution containing only  $\text{CoSO}_4$  (squares); however, the addition of trisodium citrate (CoCit -circles) shifts the reduction potential of cobalt to more negative values (-1.05 V/SCE). This shift could be attributed to the formation CoCit complexes, which cannot be reduced as easily as the free ions, requiring more negative potentials [4,19]. As Fig. 1a shows, adding  $\text{CuSO}_4$  to the solution (CoCitCu -triangles) leads to a Cu deposition peak at -0.86 V/SCE. The Cu deposition peak on Si substrate appears at (-0.55 V/SCE) (not shown). This behavior results from the formation of complexes between  $\text{Cu}^{2+}$  ions and trisodium citrate. Notably, the addition of  $\text{CuSO}_4$  to the solution brings the reduction potential of cobalt back to -0.95 V/SCE, which implies that the concentration of  $\text{Co}^{2+}$  ions increases in the solution.

Fig. 1b shows chronogalvanometric transients for films obtained by electrodeposition at -1.1 V/SCE. The cobalt films obtained with the solution containing only  $\text{CoSO}_4$  (squares) show higher current peak; however, when trisodium citrate is added to the solution (circles) the current density is reduced, as shown by the



## INTERNATIONAL JOURNAL OF RESEARCH SCIENCE & MANAGEMENT

chronogalvanometric transients. This means that the electrodeposition kinetics is reduced in the presence of trisodium citrate, in line with Fig. 1a. All films obtained with the two solutions were equally opaque and nonadherent.

When a very small amount of  $\text{CuSO}_4$  (3 mM) was added to the solution containing  $\text{CoSO}_4$  and trisodium citrate, a current increase corresponding to the formation of the first nuclei with subsequent decrease associated to the almost exclusive depletion of copper ions near the electrode. Furthermore, the copper ions are subject to overpotential even after complexation, since the potential electrodeposition of cobalt was -1.1 V/SCE. Under such circumstances a thin layer with high density of copper nuclei is formed. This layer acts as a seed layer for the growth of a cobalt-rich film. In the electrodeposition process, was observed that the current density decreases to a constant value for a considerable length of time, thus indicating growth process controlled by diffusion [3].

To determine the effective thickness of the deposits, Rutherford Backscattering (RBS) measurements were performed on the electrodeposited samples. Comparison with the nominal thickness yielded a current efficiency of 75%. The energy dispersion X-ray analysis (EDX) indicates that the cobalt-rich films obtained with the CoCitCu solution contain 4% of copper.

### 2. Morphological and structural characterization

The investigation of nucleation and growth is important to determine the morphology of the surface films, and this quantitative information was obtained with an AFM. This technique was used to assess the influence of a very small amount of copper sulfate added to the solution in the formation of films. Fig. 2 shows images of two magnetic antidot arrays obtained by NSL technique (13) in the presence and absence of the copper sulfate, respectively. As expected (see Fig. 2a) the addition of a small amount of copper sulfate to the solution contributed for a low surface roughness, allowing for a highly ordered antidot array with large scale periodicity, which was not possible to produce in the absence of copper sulfate (see Fig. 2b).

Fig. 3 shows the morphology of cobalt-rich films electrodeposited potentiostatically onto silicon (100) at -1.0 V/SCE. The thickness of the films ranged between 5 and 75 nm. The films showed homogeneous distribution of nuclei over the silicon surface. The RMS-value of surface roughness of the samples, calculated for the  $2 \mu\text{m} \times 2 \mu\text{m}$  topography scan varied between 1.6 nm and 4.0 nm for the thinner and thicker films, respectively.

Fig. 4 shows the X-ray patterns for different thicknesses of cobalt-rich films. The indexing of the peaks as reference standards was the ICDD database (00-015-0806 (fcc) and 01-071-4239 (hcp)). The percentage in Fig. 4 refers to the peak intensity in the pulverized, texture-free sample. When compared to tabulated values, the discrepant peak intensities observed indicate a strong texture in the (001) hcp and (111) fcc direction. In addition, the spectra obtained show that the films consist of a mixture of two phases (fcc and hcp), which is more evident with increasing thickness. The presence of a mixture of hcp and fcc in the cobalt-rich structure is in line with observations elsewhere [20-22]. We have identified peaks (100), (002), (101), and (110) from the hcp phase and peaks (111), (200), and (220) from the fcc phase. Due to its small thickness, the 10 nm cobalt-rich film presents clear hcp (002) and fcc (111) peaks, as well as signs of hcp (100), fcc (200), hcp (110), and (220) peaks, probably due to the absence of long-range crystalline periodicity. The presence of the fcc phase at room temperature in the electrodeposited cobalt-rich films is associated with the incorporation of atomic hydrogen in the deposits, as reported elsewhere [23-25].

### 3. Magnetic properties

The magnetic behavior of cobalt-rich films was analyzed by recorded hysteresis loops using a vibrating sample magnetometer (VSM) with magnetic field up to 10 kOe in parallel to the film plane. Fig. 5 shows the hysteresis loops for cobalt-rich films with different thicknesses. The hysteresis loops are squareness in thicker films (Fig. 6a) indicates that the easy magnetization axis is in the plane of the sample and the fast reversal of magnetization according to the applied field can be interpreted in terms of an easier rotation of domains due to the decrease in the domain wall pinning with the increasing thickness of the sample [22,26,27]. Thickness also plays an important role in the saturation magnetization of samples, which varied between 1,210-1,300  $\text{emu}\cdot\text{cm}^{-3}$  for cobalt-rich films with thickness of 20 and 75 nm. That saturation magnetization nearly corresponds to that



## INTERNATIONAL JOURNAL OF RESEARCH SCIENCE & MANAGEMENT

observed for bulk cobalt [28]. However, the saturation magnetization was of 900 and 420  $\text{emu}\cdot\text{cm}^{-3}$  for the samples of 10 nm and 05 nm, respectively. These results may be due to the predominance of copper, which is deposited preferentially in the beginning of the film growth.

Fig. 6b shows the variation of coercivity according to the thickness of cobalt-rich films. Coercivity remains constant around 20 Oe between 40 and 375 nm, which corresponds to the growth of multi domains regions. Lower coercivity is evidence of greater fcc/hcp ratio [25]. There is a quick rise in coercivity below 25 nm, peaking at a thickness of 10 nm. Within this range (10-25 nm), the very high coercivity is characterized by a single domain region. The decrease of coercivity below 10 nm may be attributed to the influence of the superparamagnetic regions [29-31].

### Conclusions

Our research has demonstrated that electrodeposition is a useful and inexpensive technique to obtain cobalt-rich films onto silicon electrodes. Electrochemical techniques suggest that the deposition of cobalt-rich film is characterized by a diffusion limited growth process. The morphology of the films observed by AFM shows a granular structure with homogeneous surface distribution, with roughness ranging from 1.6 to 4.0 nm. The X-ray patterns showed that the cobalt-rich films consisted of two phases (fcc and hcp) with strong texture in the (001) hcp and (111) fcc direction. The magnetic behavior measured by VSM indicates that the easy magnetization axis is in the plane of the cobalt-rich films and that the process of reversal magnetization is dominated mainly by domain wall pinning. The coercive field showed to be strongly dependent on the thickness of the cobalt-rich films, presenting three different regions. The first region ranged between 375-40 nm and presented constant coercivity of approximately 20 Oe; it was dominated by the growth of multi domains. The second region ranged between 40-10 nm and showed a maximum value of coercivity in approximately 10 nm that was associated to the presence of grains formed by one single magnetic domain. Finally, the third region, below 10 nm, is where there is a decrease in coercivity due to the influence of superparamagnetism.

In conclusion, the addition of a small amount of copper sulfate to the bath proved to be crucial for high quality, crack-free, adherent, smooth, bright-metallic, of the magnetic films. These qualities are particularly suitable for nanostructuring processes using nanosphere lithography.

### Acknowledgments

The authors thank the Brazilian agencies CNPq, CAPES, FAPESC and FAPESP (process 2011/11065-0) for financial support. Thank you also for the use of facilities LDRX-UFSC in X-ray diffraction and VSM experiments

**Figures:**

Fig. 1.

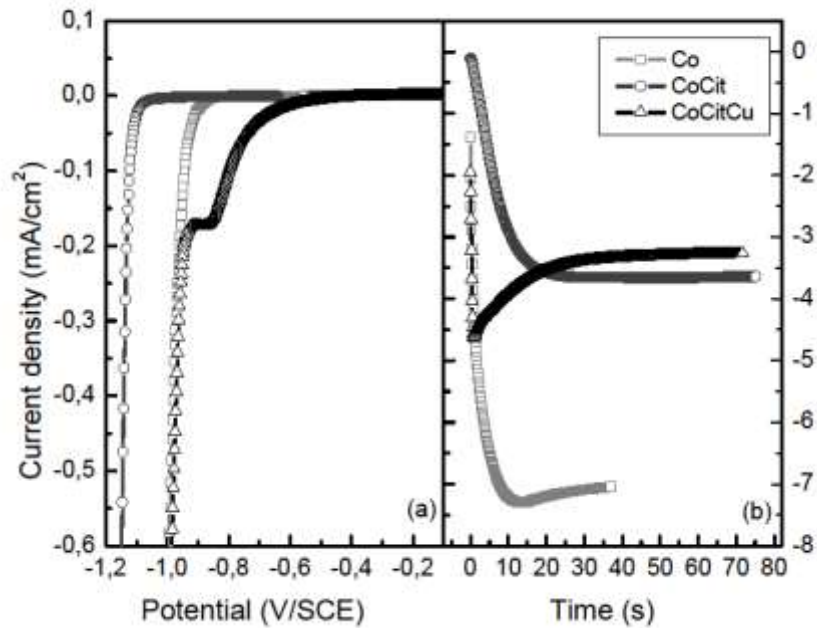


FIG. 1: Experimental data obtained at environment conditions: (a) partial cyclic voltammograms and (b) current transient for  $V = -1.1$  V/SCE and 250 mC charge deposited. Aqueous baths containing: Co (square) 300 mM of  $\text{CoSO}_4$ , CoCit(circle) 300 mM of  $\text{CoSO}_4$  + 300 mM sodium citrate and CoCitCu (triangles) 300 mM of  $\text{CoSO}_4$  + 300 mM sodium citrate +3 mM  $\text{CuSO}_4$ .



Fig. 2

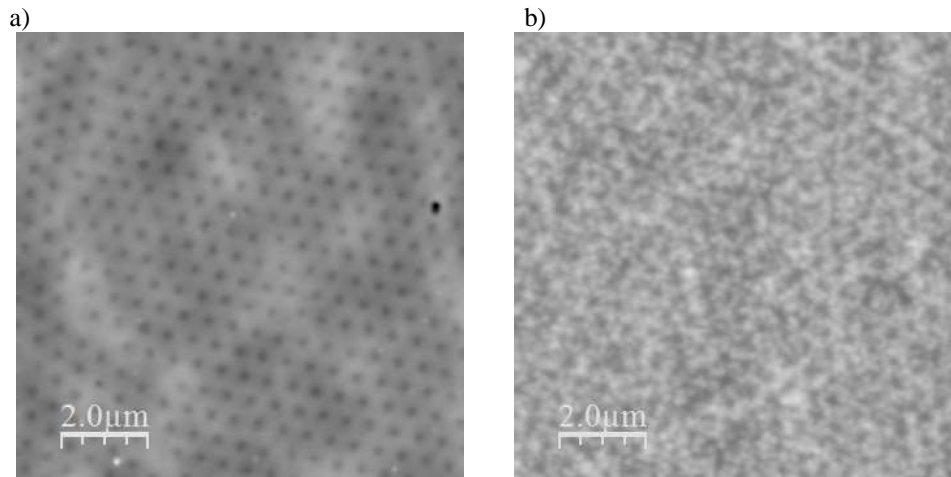


FIG. 2: AFM images electrodeposited samples through masks colloidal spheres with a diameter of 535 nm. The total deposited charge of 21mC and that the bath comprises: a) 300mM  $\text{CoSO}_4$  + 300 mM  $\text{C}_6\text{H}_5\text{Na}_3\text{O}_7$ + 3 mM  $\text{CuSO}_4$ and b) 300mM  $\text{CoSO}_4$  + 300 mM  $\text{C}_6\text{H}_5\text{Na}_3\text{O}_7$ .





Fig. 3.

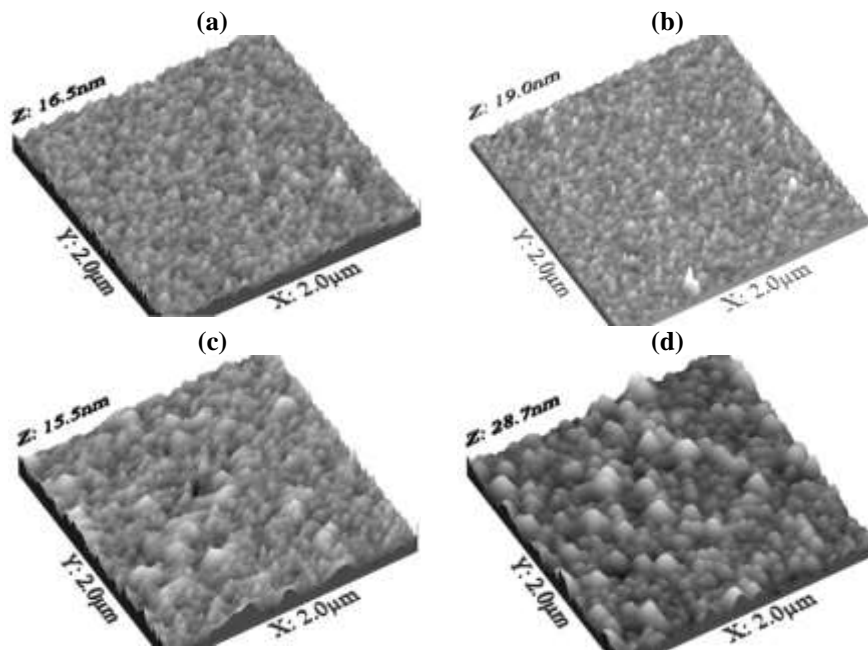


FIG. 3: AFM image (tapping-mode) for cobalt-copper deposit obtained in different thicknesses: (a) 5 nm, (b) 10 nm, (c) 20 nm, and (d) 75 nm.



Fig. 4.

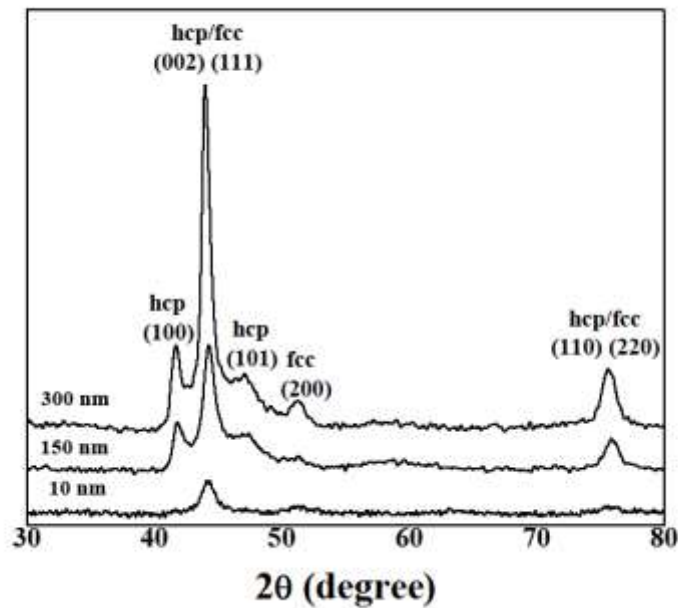


FIG. 4: XRD pattern obtained with film thicknesses of 10, 150, and 300 nm. At 150 nm and 300 nm the coexistence of fcc and hcp phases is evident by the presence of the diffraction peaks: (100) and (101) exclusively belonging to hcp phase and (200) pure fcc.





Fig. 5.

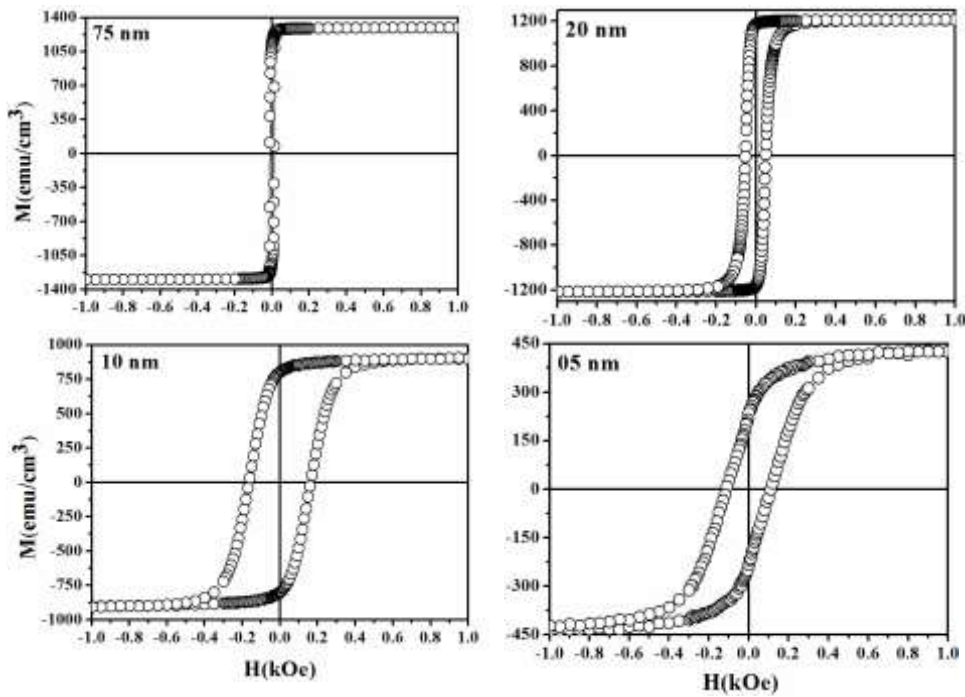


FIG. 5: Magnetic hysteresis curves recorded at room temperature with a magnetic field applied in plane for a series of cobalt-rich films with different thicknesses

Fig. 6.

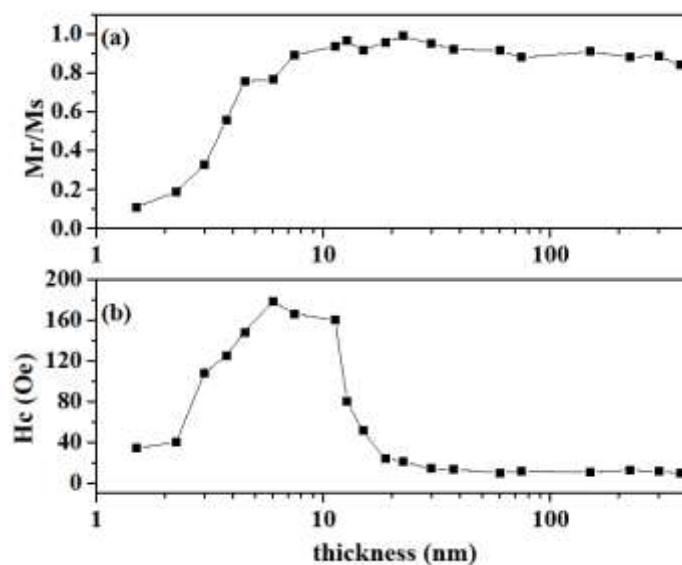


FIG. 6:(a)Use the "Insert Citation" button to add citations to this document.  $M_r/M_s$  and (b) coercive field as a function of thickness obtained for cobalt-rich films produced with the bath of 300 mM  $\text{CoSO}_4$  + 300 mM  $\text{C}_6\text{H}_5\text{Na}_3\text{O}_7$  + 3 mM  $\text{CuSO}_4$  at  $V = -1.1$  V/SCE



## INTERNATIONAL JOURNAL OF RESEARCH SCIENCE &amp; MANAGEMENT

## References

- [1] F.M. Takata and P.T.A. Sumodjo. *Electrochim. Acta.* 52(2007) 6089.
- [2] J.S. Santos, R. Matos, F. Trivinho-Strixino and E.C. Pereira. *Electrochimica Acta.* 53(2007) 644.
- [3] T.M. Manhabosco and I.L. Muller. *J. Mater. Sci.* 44(2009)2931.
- [4] S.S. Abd El Rehim, S. M. Abd El Wahaab, M. A. M. Ibrahim, M.M. Dankeria. *J Chem. Technol. Biot.* 73(1998) 369.
- [5] S.D. Bader. *Rev. Mod. Phys.* 78(2006) 1.
- [6] C. Ross. *Annu. Rev. Mater. Res.* 31(2001) 203.
- [7] L. Vila, P. Vincent, L. D. Pra, G. Pirio, E. Minoux, L. Gangloff, S. Demoustier-Champagne, N. Sarazin, E. Ferain, R. Legras, L. Piraux, P. Legagneux. *Nano Lett.* 4(2004) 521.
- [8] B. Bozzini, D. De Vita, A. Sportoletti, G. Zangari, P.L. Cavallotti and E. Terrenzio. *J. Magn. Magn. Mater.* 120(1993) 300.
- [9] T. Osaka. *Electrochim. Acta.* 45(2000) 3311.
- [10] W. Hull. *Phys. Rev.* 17(1926) 571.
- [11] E. Gomez and E. Valles. *J. Appl. Electrochem.* 32(2002) 693.
- [12] Q. Zhou, P.J. Heard and W. Schwarzacher. *J. Appl. Phys.* 109(2011) 054313.
- [13] E.R. Spada, A.S. Rocha, E.F. Jasinski, G.M.C. Pereira, L.N. Chavero, A.B. Oliveira, A. Azevedo and M.L. Sartorelli. *J. Appl. Phys.* 103(2008) 114306.
- [14] E.R. Spada, G.M.C. Pereira, E.F. Jasinski, A.S. da Rocha, O.F. Schilling, M.L. Sartorelli. *J. Magn. Magn. Mater.* 320(2008) E253.
- [15] L. J. Heyderman, F. Nolting, D. Backes and S. Czeka. *Phys. Rev. B.* 73(2006) 12.
- [16] C.C. Wang, A.O. Adeyeye and N. Singh. *Appl. Phys. Lett.* 88(2006) 222506.
- [17] M.T. Rahman, R.K. Dumas, N. Eibagi, N.N. Shams, Y.C. Wu, K. Liu and C.H. Lai. *Appl. Phys. Lett.* 94(2009) 42507.
- [18] T. Wang, Y. Wang, Y. Fu, T. Hasegawa, H. Oshima, K. Itoh, K. Nishio, H. Masuda, F.S. Li, H. Saito and S. Ishio. *Nanotechnology*, 19(2008) 455703.
- [19] N.C. Li, A. Lindenbaum and J.M. White. *J. Inorg. Nucl. Chem.* 12 (1959) 122.
- [20] A. Azizi, A. Sahari, M.L. Felloussia, G. Schmerber, C. Mény and A. Dinia. *Appl. Surf. Sci.* 228(2004) 320.
- [21] M. Cerisier, K. Attenborough, E. Jedryka, M. Wojcik, S. Nadolski, C. Van Haesendonck and J. P. Celis. *J. Appl. Phys.* 89(2001)7083.
- [22] M.L. Munford, L. Seligman, M.L. Sartorelli, E. Voltolini, L.F.O. Martins, W. Schwarzacher, A. A. Pasa. *J. Magn. Magn. Mater.* 226(2001)1613.
- [23] M. Cerisier, C. Van Haesendonck, J.P. Celis. *J. Electrochem. Soc.* 146(1999)1829.
- [24] M. Cerisier, K. Attenborough, J.-P. Celis, C. Van Haesendonck. *Appl. Surf. Sci.* 166(2000) 154.
- [25] S. Armyanov. *Electrochim. Acta.* 45(2000)3323.
- [26] H.-G. Min, S.-H. Kim, M. Lib, J.B. Wedding, G.-C. Wang. *Surf. Sci.* 400(1998)19.
- [27] H. Wan, G.C. Hadjipanayis. *J. Appl. Phys.* 70(1991)6059.
- [28] C. Chappert, P. Bruno. *J. Appl. Phys.* 64 (1988) 5736.
- [29] J.S. Judge, J.R. Morrison, D.E. Speliotis and G. Bate. *J. Electrochem. Soc.* 112(1965) 681.
- [30] Cullity, B.D., *Elements of X-ray Diffraction.* second ed. (1978).
- [31] J. Camarero, J.J. de Miguel, R. Miranda and A. Hernando. *J. Phys-Condens. Mat.* 12(2000) 7713.